Wear 270 (2011) 876–887

Contents lists available at ScienceDirect

Wear

journal homepage: www.elsevier.com/locate/wear

Numerical simulation of the third body in fretting problems

Stéphanie Basseville [a,*], Eva Héripré [b], Georges Cailletaud [c]

[a] LISV, Universitĭe de Versailles Saint-Quentin, 45 avenue des Etats-Unis, 78000 Versailles, France
[b] Laboratoire de Mĭecanique des Solides, Ecole Polytechnique, 91128 Palaiseau Cedex, France
[c] MINES ParisTech, Centre des Matĭeriaux, CNRS UMR 7633, BP 87 91003 Evry Cedex, France

ARTICLE INFO

Article history:
Received 5 March 2010
Received in revised form 16 February 2011
Accepted 17 February 2011
Available online 24 February 2011

Keywords:
Finite elements
Third body
Fretting
Dang Van's fatigue model
Wear

ABSTRACT

This study is devoted to the computation of realistic stress and strain fields at a local scale in fretting. Models are proposed to improve surface and volume modelling, by taking into account the *heterogeneity* of stress fields due to the irregular interface. This gives a new view toward damage mechanisms. The surface heterogeneity which is considered here, results from the third body trapped in the contact zone. This third body is known to drastically influence the contact conditions. The competition between wear and crack initiation is investigated with respect to local stress fields. The first model is used to study the evolutions of particles and the contact stress according to the loading conditions. Then, Dang Van's multiaxial fatigue model is used to predict crack initiation during the fretting test. This criterion may highlight the presence of microcracking everywhere in the contact zone.

1. Introduction

Damage prediction in contact areas submitted to fretting is an serious issue, since it is often a limiting factor for the design of industrial components. Most of the papers in the literature consider a comprehensive approach of this problem, and use pure macroscopic models to evaluate the stress and strain fields at the contact surfaces [1,2]. This does not take into account the fact that, in contact problems, the volume of material enduring critical load levels is remarkably small, i.e. much less than a cubic millimeter. This size may be comparable to the size of several grains only in metallic alloys and/or particles that could be trapped in the contact zone. Thus, they probably have an impact in the prediction of the fretting damage, and they must be introduced in the modelling.

The aim of this paper is to propose solutions to take into account the heterogeneous character of the material, and to show that the mechanism change can be captured by simple critical variables at a local scale in the FE computation to point out the consequences for life predictions. In fretting contacts, wear and fatigue mechanisms interact, so one has to consider these two phenomena simultaneously. At low-displacement amplitudes in partial slip, fatigue dominates, whereas wear prevails at large displacement amplitudes in gross slip [3]. The concept of fretting map is used to define the conditions for which each damage mechanism is predominant as described in section 2 for cylinder–plate tests performed on titanium alloys. Some wear mechanisms, such as adhesion and oxidation, might promote fatigue in partial slip [4]. In the gross slip conditions, wear can prevent fatigue damage to occur by eliminating surface cracks at a faster rate than their growth [5].

Due to the complexity of the sliding surface interaction, literature presents many models about these damage mechanisms. More than one hundred wear models are listed in [6]. Nevertheless, Archard's law [7] often inspires wear modelling and it has been adapted to fretting wear in finite element (FE) analysis [8–10]. In this study, the wear model is based upon the Oqvist's approach [8] as described in Section 4. The model explicitly includes the third body which is known to drastically affect the contact conditions. Oqvist's model has been adapted to represent the matter transfer towards the third body.

A literature review on fretting fatigue modelling can be found in [4]. These last years, applications of multiaxial fatigue parameters [11,12], fracture mechanics [13] and fatigue mechanics [2,14] to fretting contact problems have been developed. Some other authors have studied the role of material modelling in fretting fatigue prediction [1,15,16]

In our study, it has been decided to use Dang Van's multiaxial fatigue model to predict crack initiation during a cylinder–plate fretting test. The definition of this model is recalled in Section 3. The important problem of the description of the third body is considered here. It is known to drastically influence the contact conditions. An attempt to develop an original description of this material is then presented in Section 4. It allows to predict the cap-

* Corresponding author. Tel.: +33 1 39 25 30 15.
E-mail addresses: stephanie.basseville@uvsq.fr (S. Basseville), heripre@lms.polytechnique.fr (E. Héripré), georges.cailletaud@mines-paristech.fr (G. Cailletaud).

0043-1648/$ – see front matter © 2011 Elsevier B.V. All rights reserved.
doi:10.1016/j.wear.2011.02.016

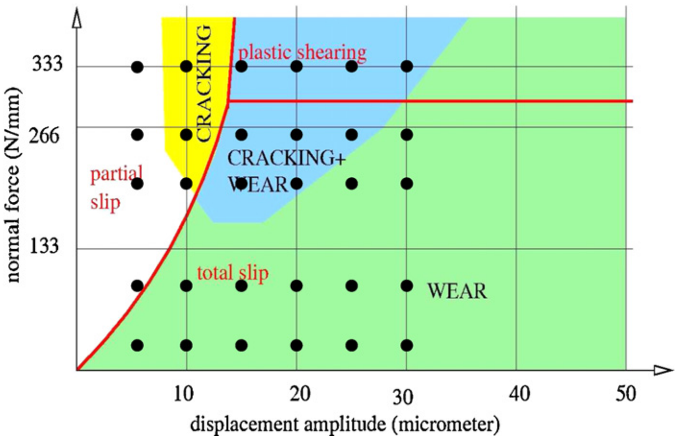

Fig. 1. Material response fretting map as determined by [20]. The loading conditions of the computations performed in our study are indicated by black points in the diagram.

ture of the matter inside the contact or its ejection in relation with the loading conditions (Section 5). Its influence on wear and fatigue life prediction is evaluated here and compared to FE computation without considering the third body.

2. A material response fretting map

The concept of fretting map, already approached in the past [17] has been introduced by [18,19] to underline the relation between the transition from partial slip to gross slip and the transition from crack initiation to wear. It has been recently applied to titanium alloy (Ti6Al4V) which is chosen as an example in this study [20]. The corresponding response is drawn for 10^6 cycles (Fig. 1) of a cylinder/plate fretting test. The cylinder radius is equal to 10 mm. Depending on the displacement amplitude and the normal load, one of these responses is observed: *no damage*, *fatigue cracking*, *fatigue cracking and wear* or *wear* only. These four domains are indicated in the material response fretting map (Fig. 1). By means of linear elastic computations, the field can be splitted into a partial slip and a total slip domain. In elastic–plastic computations, an additional domain can be found where the relative displacements between the bodies are not accommodated by contact sliding but by near surface material flow. The horizontal boundary indicated in Fig. 1 marks the onset of large plastic flow.

In the partial slip domain, no damage is obtained in experiment with low normal forces (133 MPa). At higher normal forces (266 MPa, 333 MPa), cracks have been detected in tests with sufficiently high displacement amplitude. In the total slip regime, wear is the only damage mechanism for low normal forces (133 MPa). At higher normal forces (266 MPa, 333 MPa), wear and cracking are both detected for lower displacement amplitudes, and only wear for higher displacement amplitudes.

Adhesion is the main source of wear at low normal forces so that the strain fields predicted with models using a von Mises criterion are not relevant to fully explain the wear process. When a microstructural scale material model is introduced, larger local strains will be produced, due to a series of localization problems that cannot be observed with classical plasticity models. This effect is of increasing importance with increasing normal force – then plasticity related wear may be predominant, and may hide the phenomena linked to adhesion. The deepest cracks in fretting tests are obtained in the "partial slip regime" where wear is also observed.

3. Material modelling

TA6V is a near α titanium base alloy. In the present state, it is made of 50% lamellar packs of HCP α-phase and bcc β-phase and 50% α grains with a grain size of 30 μm. On the whole the β-phase does not constitute more than a few percent in this alloy. A crystallographic texture is present at two scales. The material exhibits a macro texture. A preferential orientation of all the grains is present at a macroscale. Additionally, a micro texture has been observed. The domains of neighbouring grains have a very similar orientation constituting super grains [21]. Some qualitative information about the macro texture of the material can be found in [22]. The main texture is caused by a preferential orientation of the *c*-axis of the hexagonal lattice in the normal direction (ND) of the specimen whereby uniaxial tests with an imposed deformation in the "rolling direction" (RD) were made. The elastic constants are respectively 119 GPa for the Young's modulus and $\nu = 0.29$ for Poisson's ratio. The elastic limit is $R_p^{0.2} = 850$ MPa and the tensile strength R_m is around 1000 MPa. For cyclic material modeling a phenomenological "von Mises" approach [2] was applied. All material parameters were identified using cyclic fatigue tests under deformation control at $R_\varepsilon = \varepsilon_{\min}/\varepsilon_{\max} = -1$.

As a first approach, we restrict ourselves to elastic computations. The applications will show that the von Mises stress remains below or just above the yield stress even in the contact area.

The classical version of Dang Van's criterion introduces a combination of the actual shear stress and hydrostatic pressure, *P*. For a given facet, characterised by its normal $\vec{n}$, the circle that encloses the shear path described during one cycle is defined. The shear $\tau_{\vec{n}}(t)$ that is used in the criterion is the distance between the current point of the shear path and the center of this circle. For a given time *t*, one of the facet presents the highest value of the linear combination of $\tau_{\vec{n}}(t)$ and $P(t)$, called equivalent Dang Van's stress, $\sigma_{DV}(t)$. The path in the P–τ plane should remain in the half space where this stress remains smaller than a critical value, that is nothing but the fatigue limit in pure shear, τ_0.

$$\sigma_{DV}(t) = \max_{\vec{n}}(\tau_{\vec{n}}(t) + bP(t)) \tag{1}$$

$$f(\sigma) = \max_{t}\sigma_{DV}(t) - \tau_0 \tag{2}$$

The material parameters b and σ_0 are constants that have to be calibrated from two independent tests, either pure tension and shear fatigue, or two tensile tests with different R ratios ($R = \sigma_{\min}/\sigma_{\max}$).

In the present application, an alternative formulation is used. The Tresca type shear is replaced by a von Mises evaluation. The load path is considered in the tensorial stress space, and one search for the hypersphere that encloses the full path. Its center is a deviatoric tensor. The actual shear at time *t* does not introduce any facet definition. It is just computed as the distance in the deviatoric stress space between the current point of the cycle and the previously defined center, denoted by J^*. Following the previous case, a linear combination is introduced between J^* and the trace I_1 of the stress tensor, $I_1(t) = \mathrm{Trace}(\underset{\sim}{\sigma})(t)$. The computation of the criterion is much faster in this case, since there is no facet. As a drawback, there is no more information concerning the orientation of the crack initation plane.

$$\sigma^*_{DV}(t) = (1 - b^*)J^*(t) + b^* I_1(t) \tag{3}$$

$$f^*(\sigma) = \max_{t}\sigma^*_{DV}(t) - \sigma^*_0 \tag{4}$$

With the shape chosen in Eq. (3), crack initiation occurs when the critical stress reaches the fatigue limit σ_0 in pure tension under reverse loading $R = -1$. As an example, the maximum values of $\sigma^*_{DV}(t)$ are respectively: